[11] A-Kaymam, 209 CL.

Notes for Lecture #3
PWM Inverters.

8

Sequential Method of Simulation of Power Electronic Systems

8.0 INTRODUCTION

Our earlier analysis of power electronic converter systems composed of a static power converter, an electrical machine, and associated control strategy was done using global simulation programs such as ATOSEC5, SACSO, and SACMA [1-3]. In these computer-aided analysis simulation programs, no prior knowledge of the sequence of operation of the converter was assumed. For the study, we had to know the circuit topology of the converter, the type of electrical machine, and the control logic for the turn-on instants of the controlled semiconductors. In this chapter we discuss another method of simulation called the sequential method. In this method, as the name suggests, the sequence of operation of the power converter

is assumed to be known; further, the time instants at which the change of sequence occurs is also assumed to be known. This implies that in one class of problems, the output voltages or currents of the power converter are known to be independent of the operating modes of the electrical machine. We refer to this class of systems as decoupled systems. In other words, the analysis of the system can be reduced to the analysis of the electrical machine fed from nonideal sources, such as pulsed sources for dc machines and nonsinusoidal voltage or current sources for ac machines. In another class of problems, only the sequence of operation of the converter is known, although the instants at which the change of sequence occurs might have to be determined during the analysis. We refer to this class of systems as coupled systems. We discuss both these methods of analysis in this chapter.

8.1 DECOUPLED AND COUPLED POWER ELECTRONIC SYSTEMS

Consider the power electronic system consisting of a three-phase line-commutated converter and a dc machine shown in Fig. 8.1. The control strategy used is such that the six thyristors of the converter are turned on at a constant phase-angle delay in order to obtain a rectifying mode of converter operation. A simplified analysis of this converter in the rectifying mode is well known [4]. The sequence of firing of the thyristors is shown in Fig. 8.1. The analysis of the dc motor fed from the converter can easily be done if we assume that the commutation overlap

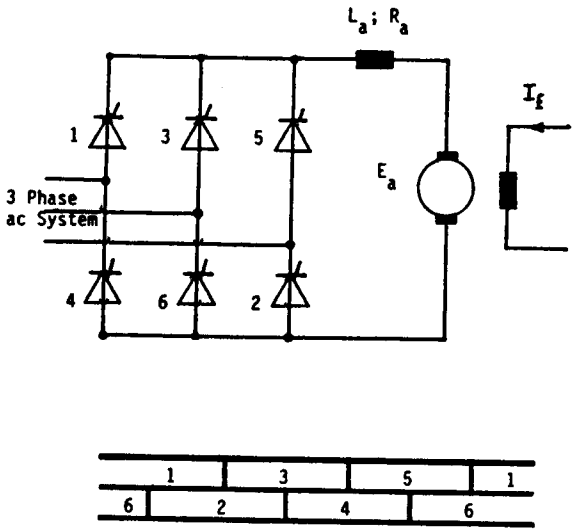

FIGURE 8.1 Dc drive system.

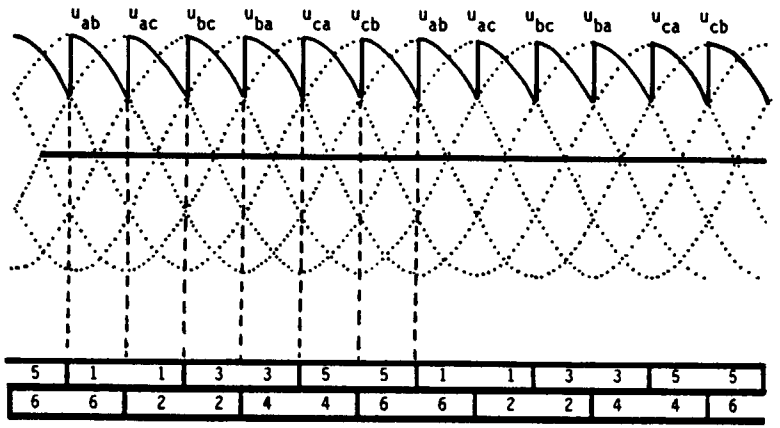

FIGURE 8.2 Output voltage of a three phase line-commutated converter assuming instantaneous commutation.

angles are neglected. In other words, the output voltage of the converter can be assumed to be as shown in Fig. 8.2 if the commutation is instantaneous. It is thus possible to decouple the converter operation from the electrical machine. The analysis of the system is therefore simplified to one in which a nonideal dc voltage source such as the one shown in Fig. 8.2 is used to feed the dc machine. Note that the voltage drops due to the source resistance and inductance are taken into account indirectly by adding an equivalent series resistor at the output side of the converter.

Let the commutation interval of the converter be considered for the system. It is well known that the commutation overlap angle depends on the value of the instantaneous current to be commutated. To analyze this operating condition, we utilize the coupled system, where only the turn-on instants of the thyristors are known. The sequence of operation of the different thyristors is shown in Fig. 8.3, which indicates an operating sequence 1-2, 1-2-3, 2-3, 2-3-4, 3-4, 3-4-5, 4-5, 4-5-6, 5-6, 5-6-1, 6-1, 6-1-2, 1-2, and so on. The output voltage waveform is

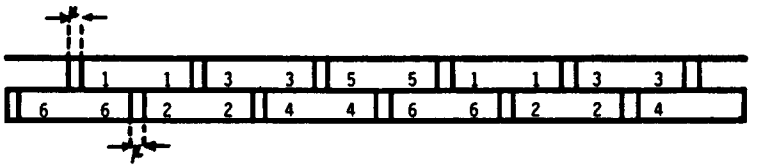

FIGURE 8.3 Sequence of operation of thyristors in a three phase converter with commutation overlap angle μ.

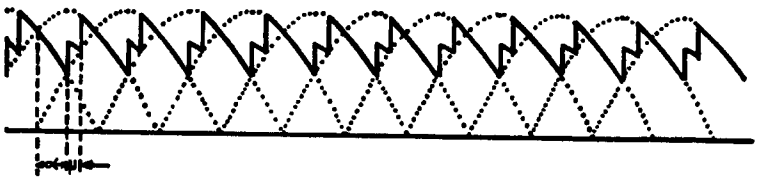

FIGURE 8.4 Output voltage of a three phase line-commutated converter-commutation overlap angle μ.

only partially defined because the instants at which the change of sequence from 1-2-3 to 2-3, and so on, occurs are unknown and have to be computed during the analysis. The typical output waveform is shown in Fig. 8.4. This class of systems are coupled systems.

EXAMPLE 8.1. Consider the chopper-fed dc machine shown in Fig. 8.5. Discuss how the analysis of the system can be done assuming a decoupled system.

Solution: The operating sequence of the chopper system is well known [5] and can easily be established by reference to Fig. 8.5. The conduction of thyristor T_M supplies a source voltage V_d to the armature of the dc machine. Assuming an initial voltage of suitable polarity across the commutating capacitor C_c, turning on

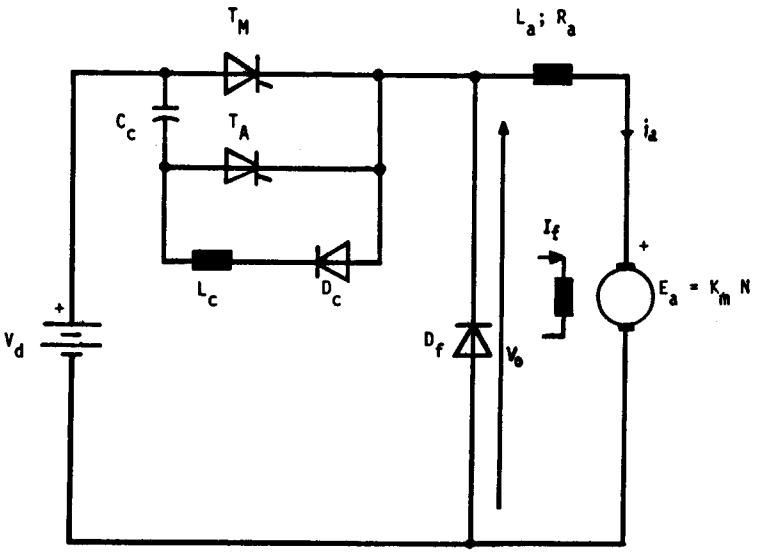

FIGURE 8.5 Chopper-fed dc machine.

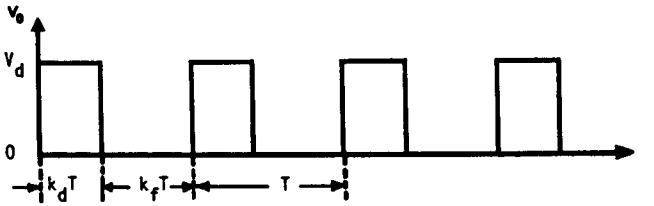

FIGURE 8.6 Output voltage of the dc chopper with negligible commutation interval.

the auxiliary thyristor, T_A, results in turning off the main thyristor by the application of an inverse voltage across the main thyristor. Assuming that this commutation period is negligible, the output waveform of the chopper circuit can be determined independent of the operating mode of the dc machine. The system can then be analyzed as a decoupled system. That is, the output voltage waveform of the chopper is a pulsed dc voltage, as shown in Fig. 8.6. The ratio between the conduction interval of the main thyristor and the period of the chopper is designated as the duty cycle (D) of the chopper.

8.2 ANALYSIS OF DECOUPLED SYSTEMS

8.2.1 Analysis of Chopper-Fed DC Motor

Various methods are available for obtaining a variable dc voltage from a constant dc source [6]. In thyristor-type dc-to-dc converters, commutating circuits are required which are similar to those used in many inverters. A classical chopper scheme employing an impulse commutation technique is chosen for our study [7]. A fixed frequency modulation is used for the chopper circuit, because in this scheme, harmonics of a particular frequency alone will occur and can easily be filtered. The variable dc voltage available from the chopper is used to feed the armature of the dc motor with separate excitation, thus controlling the speed of the motor. An inductor has been introduced in the armature circuit to reduce the armature current ripples. In what follows, a chopper-fed dc motor group is analyzed and the steady-state performance characteristics of the dc motor are obtained.

Figure 8.7 shows a dc-to-dc converter and the associated control logic signals for firing of the thyristors. The operating sequences of the converter are characterized by four intervals: precharging interval, duty interval, commutation interval, and freewheeling interval.

PRECHARGING INTERVAL. The control logic used here is such that initially, only the auxiliary thyristor, T_A, is turned on periodically; the commutating capacitor C_c is allowed to get charged to a voltage equal to the dc voltage source. The polarity of the voltage across the commutating capacitor is such that point A in Fig. 8.7 is more positive than point B. This precharging interval is essential to ensure proper commutation in the chopper circuit. Normally, the operating cycle of the chopper consists of a duty interval, a commutation interval, and a freewheeling interval.

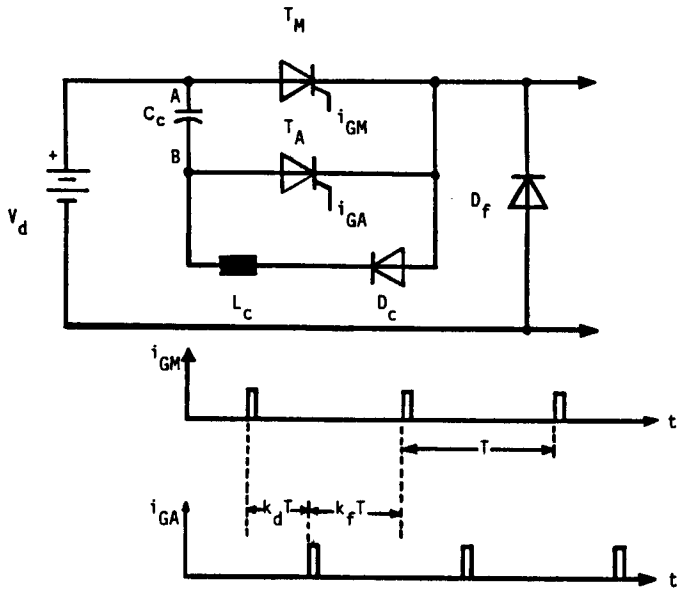

FIGURE 8.7 Dc to dc converter and associated control logic.

DUTY INTERVAL. With the firing of main thyristor, T_M, the duty interval begins and the dc source voltage appears across the dc motor, assuming a negligible forward voltage drop across the main thyristor. The capacitor voltage reverses its polarity and attains the same magnitude at the end of a half-period of the resonant circuit constituted by L_c, C_c, and negligible resistance. Any further discharge of the capacitor is prevented by the blocking diode, D_c, connected in series with the commutating inductor, L_c. As soon as the auxiliary thyristor, T_A, is turned on, the commutation interval begins and the duty interval terminates.

COMMUTATION INTERVAL. The firing of the auxiliary thyristor marks the beginning of the commutation interval. The load current flowing through the main thyristor is transferred to the commutating capacitor and the auxiliary thyristor. The capacitor voltage is applied across the anode-cathode terminals of the main thyristor as an inverse voltage. It is necessary that this inverse voltage be applied across the main thyristor for at least the turn-off time of the main thyristor. The capacitor gets charged from the dc source through the load and changes its polarity. The commutation interval can last until the capacitor gets charged to a voltage equal to the source voltage or can terminate when the main thyristor is refired. In the former case, the capacitor voltage can have a tendency to get charged to a voltage greater than the source voltage in inductive and emf types of loads. Such a tendency initiates conduction of the freewheeling diode D_f, which marks the beginning of the freewheeling interval. In the latter case, where the commutation

interval is terminated by refiring of the main thyristor even before the capacitor voltage has attained the supply voltage value, there results a reduced voltage available for commutation of the main thyristor in the next cycles of operation. It can therefore be noted that commutation failure is bound to occur as the duty interval approaches the period of the chopper. Commutation failure results in permanent conduction of the main thyristor, and the control over duty interval can be regained only after opening of the load circuit followed by a precharging interval.

FREEWHEELING INTERVAL. During this interval, the load current is transferred through the freewheeling diode and the dc motor armature circuit. In the case of emf loads, this interval terminates as soon as the load current falls below a value leading to blocking of the freewheeling diode or as soon as the main thyristor is turned on. The former case occurs when the motor is lightly loaded, as the duty cycle is low. This results in a discontinuous armature current; otherwise, the armature current is continuous.

STEADY-STATE ANALYSIS OF THE CHOPPER-FED DC MOTOR WITH SEPARATE EXCITATION. For purposes of analysis, the following assumptions are made:

1. The armature circuit resistance R_a is constant.
2. The inductance L_a of the armature circuit is constant.
3. The speed N of the motor is constant.
4. The forward voltage drops of semiconductor elements and the source impedance are neglected.
5. The field of the motor is separately excited and the flux is constant.

Let the armature current at the end of the duty interval be I_d and let its value at the end of the commutation and freewheeling intervals be I_c and I_f, respectively. Let N be equal to the speed of the motor. Since the field is excited from a constant separate dc source, the induced emf is proportional to the speed of the motor. Our objective is to find the average value of the armature current for given values of speed N and known values for the various intervals.

The differential equations governing the commutation, duty, and freewheeling intervals of the chopper-fed motor group can now be formulated.

COMMUTATION INTERVAL $0 < t \leq k_cT$. Let the instantaneous armature current during the commutation interval be designated as i_c. The equations governing this interval are

$$V_d = R_a i_c + L_a \frac{di_c}{dt} + K_m N + v_c \tag{8.1}$$

$$C_c \frac{dv_c}{dt} = i_c \tag{8.2}$$

where

K_m = back emf constant for the dc motor

v_c = instantaneous voltage across the commutating capacitor

The initial conditions for the capacitor voltage and the armature currents are defined by

$$v_c|_{t=0} = -V_{cf} \tag{8.3}$$

$$i_c|_{t=0} = I_d \tag{8.4}$$

Let the final values of v_c and i_c at the end of the commutation interval be defined as given in

$$v_c|_{t=k_cT} = V_{cf} \tag{8.5}$$

$$i_c|_{t=k_cT} = I_c \tag{8.6}$$

Solutions for i_c and v_c can be written

$$i_c = I_{c1} \exp(-\beta t) \sin \omega t - I_d \frac{\omega_0}{\omega} \exp(-\beta t) \sin(\omega t - \phi) \tag{8.7}$$

$$v_c = V_d - K_m N - V_{c1} \frac{\omega_0}{\omega} \exp(-\beta t) \sin(\omega t + \phi) + \frac{I_d}{\omega C_c} \exp(-\beta t) \sin \omega t \tag{8.8}$$

where

$$\begin{aligned} I_{c1} &= (V_d - K_m N + V_d)/\omega L_a \\ V_{c1} &= V_d - K_m N + V_d \\ \omega_0^2 &= 1/L_a C_c \\ \beta &= \sqrt{R/2L_a} \\ \omega^2 &= \omega_0^2 - \beta^2 \\ \phi &= \tan^{-1}(\omega/\beta) \end{aligned} \tag{8.9}$$

exp = exponential operation

If the losses in the circuit are relatively small, then $\omega_0 \gg \beta$ and the simplifications given below are valid:

$$\omega_0 \simeq \omega$$

$$X = \sqrt{\frac{L_a}{C_c}} \simeq \omega L_a \simeq \frac{1}{\omega C_c}$$

$$Q = \frac{X}{R_a}$$

$$\phi \simeq \frac{\pi}{2}$$

Equations (8.7) and (8.8) can be simplified as follows:

$$i_c \simeq (I_{c1} \sin \omega t + I_d \cos \omega t) \exp\left(\frac{-\omega t}{2Q}\right) \tag{8.11}$$

$$v_c \simeq V_d - K_m N + (XI_d \sin \omega t - V_{c1} \cos \omega t) \exp\left(\frac{-\omega t}{2Q}\right) \tag{8.12}$$

Equations (8.11) and (8.12) describe the performance of the converter and the dc motor during the commutation interval. We derive next the equations governing the performance of the system during the freewheeling interval.

FREEWHEELING INTERVAL $k_cT < t \leq (k_c + k_f)T$. The condition for the existence of this interval is derived from the final value of the capacitor voltage at the end of the commutation interval. This is given by

$$V_{cf} = V_d \tag{8.13}$$

That is, this interval exists only if the commutating capacitor tends to get charged to a value greater than that of the dc source voltage. The load current circulates only through the armature and the freewheeling diode; the equation governing the operation of the system is

$$R_a i_f + L_a \frac{di_f}{dt} + K_m N = 0 \tag{8.14}$$

The initial and final conditions for the freewheeling load current i_f are defined by

$$\begin{aligned} i_f|_{t=k_cT} &= I_c \\ i_f|_{t=(k_c+k_f)T} &= I_f \end{aligned} \tag{8.15}$$

The solution for the freewheeling current i_f is given by

$$i_f = \frac{-K_m N}{R_a}\left\{1 - \exp\left[\frac{R_a}{L_a}(-t + k_cT)\right]\right\} + I_c \exp\left[\frac{R_a}{L_a}(-t + k_cT)\right] \tag{8.16}$$

The freewheeling interval is terminated when the load current becomes zero or when the main thyristor is turned on.

DUTY INTERVAL $(k_c + k_f)T < t \leq T$. The load current i_d during the duty interval is described by

$$R_a i_d + L_a \frac{di_d}{dt} + K_m N = V_d \tag{8.17}$$

The initial and final conditions of current are given by

$$i_d|_{t=(k_c+k_f)T} = I_f \tag{8.18}$$

$$i_d|_{t=T} = I_d \tag{8.19}$$

The following equation implies that the steady-state solution is reached:

$$i_d|_{t=T} = i_c|_{t=0} \tag{8.20}$$

Using the relation given by Eq. (8.20), the solution for the load current during the duty interval can be obtained:

$$i_d = \frac{V_d - K_m N}{R_a} [1 - \exp(T_d)] + I_f \exp(T_d) \tag{8.21}$$

where

$$T_d = \frac{R_a}{L_a} [-t + (k_c + k_f)T]$$

Let us analyze the operation of the chopper-motor group assuming that the load current is continuous. Further, for low values of the duty cycle k_d, the magnitude of the initial capacitor voltage is equal to the dc source voltage. The initial current I_d is to be calculated by an iterative procedure satisfying the differential equations for the three intervals with the various boundary conditions. Four different methods are discussed in the literature [6] for the calculation of I_d, I_c, and I_f without resorting to an iterative procedure. The average value of the armature current can then be computed as a function of speed. These methods are based on the following assumptions:

Method 1: negligible commutation interval
Method 2: negligible ripple in the armature current
Method 3: constant current during commutation
Method 4: relatively small losses in the commutating circuit

The assumption of a negligible commutation interval enables the study of the system as a decoupled system.

METHOD 1: STUDY OF THE DECOUPLED SYSTEM. The assumption of a negligible commutation interval leads to a decoupled system. The following equations hold good under this condition:

$$k_c = 0 \quad I_c = I_d \tag{8.22}$$

Using Eqs. (8.16) and (8.21), we can derive

$$i_f = \frac{-K_m N}{R_a} \left[1 - \exp\left(\frac{-t}{T_e}\right)\right] + I_d \exp\left(\frac{-t}{T_e}\right) \tag{8.23}$$

$$i_d = \frac{V_d - K_m N}{R_a} \left[\left(1 - \exp \frac{-t + k_f T}{T_e}\right)\right] + I_f \exp\left(\frac{-t + k_f T}{T_e}\right) \tag{8.24}$$

$$I_f = \frac{V_d}{R_a} \frac{\exp(k_d T/T_e) - 1}{\exp(T/T_e) - 1} - \frac{K_m N}{R_a} \tag{8.25}$$

$$I_d = \frac{V_d}{R_a} \frac{1 - \exp(-k_d T/T_e)}{1 - \exp(-T/T_e)} - \frac{K_m N}{R_a} \tag{8.26}$$

$$I_{av} = \frac{V_d k_d - K_m N}{R_a} \tag{8.27}$$

The average value of the torque developed by the motor is given by

$$T_{em} = \frac{60 K_m I_{av}}{2\pi} \tag{8.28}$$

The waveforms predicted for the armature current and the chopper output voltage are shown in Fig. 8.8.

Analysis of the chopper-fed dc motor based on the other simplified assumptions (methods 2, 3, and 4) described above is left as a series of exercises to the reader. The torque-speed characteristics of the chopper-fed dc motor obtained by the four methods are shown in Fig. 8.9. In Fig. 8.9, different values of the duty cycle k_d have been assumed for the computation. The experimental measurement of the test points are also indicated on Fig. 8.9.

For experimental verification of the four methods of analysis, tests were conducted on a 1.5-kW 220-V dc motor with separate excitation. The field current of the motor was maintained constant at its rated value of 3.7 A. A 200-mH choke coil was included in the armature circuit for smoothing the armature current waveform. Three sets of experiments were conducted for values of k_d = 0.11, 0.32, and 0.45, with the input voltage of the chopper maintained constant at 200 V. The relevant details of the chopper-motor group are as follows:

V_d = 200 V T = 6.67 ms L_a = 200 mH C_c = 20 μF R_a = 5 Ω

T_e = 40 ms K_m = 0.1435 V/rpm nominal speed N_e = 1392 rpm

nominal torque T_e = 10 N·m

In each experiment, the load was varied and the average torque and speed were measured. Figure 8.9 shows these characteristics. Waveforms of the armature current observed during the test conditions showed that there was a continuous conduction in the armature current.

From the characteristics it is seen that the assumption of negligible commutation (method 1) leads to a very simple expression for the torque-speed relationship, but the prediction is very much in error; this method underestimates the torque-developing capability of the dc motor. Further, this assumption is not justified, because the commutation interval varies over a wide range depending on the loading conditions of the motor. The commutation interval is, in general, comparable to the duty interval even under the heavily loaded conditions of the motor. Except for loads where the speed factor, N/N_e, approaches unity, the test points lie more-or-less midway between the curves that have been predicted using method 3 and method 2. In general, method 4 predicts the characteristics that are in reasonable agreement with experimental values. However, a relatively large deviation is noted in the values corresponding to heavily loaded conditions of the motor. Better agreement between experimental and computed results from method 4 could be expected if the increased value of the apparent resistance of the armature due to the high-frequency pulsating current is used in place of the dc value in the equations. A method of measuring the apparent resistance of the

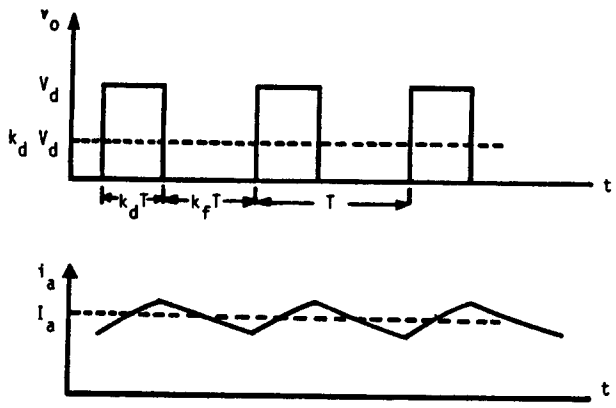

FIGURE 8.8 Chopper output voltage and armature current waveforms—Method 1.

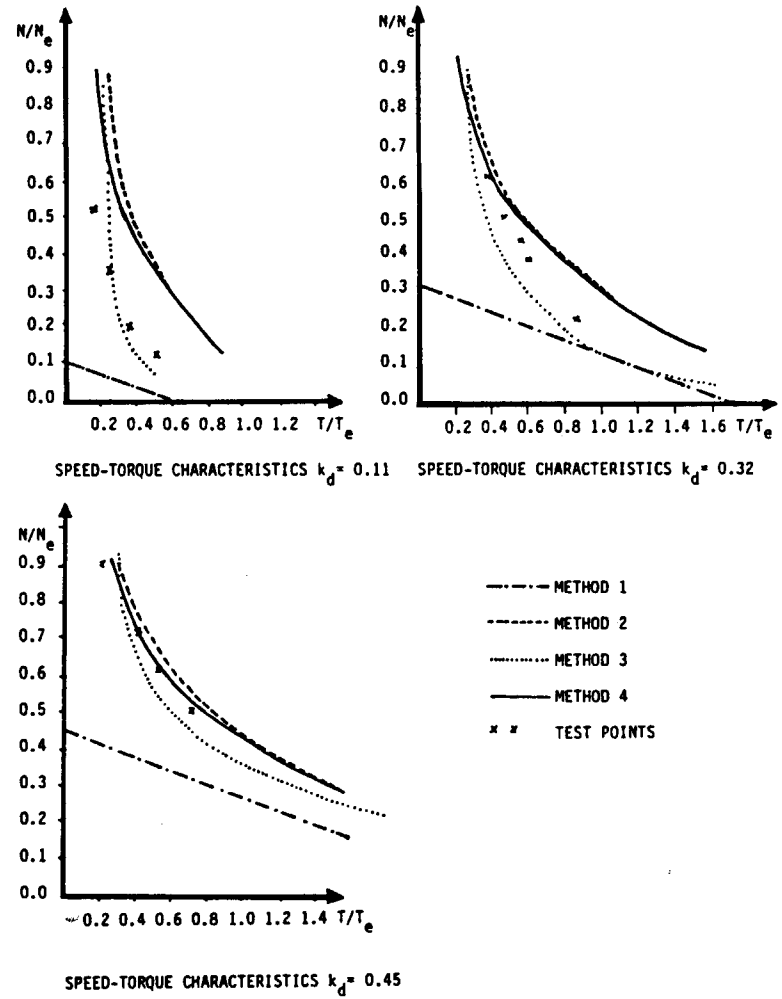

FIGURE 8.9 Speed-torque characteristics of chopper-fed dc motor.

armature circuit is suggested in the literature [5]. The speed-torque characteristics of the dc drive system, taking into account the apparent resistance, are shown in Fig. 8.10. For this computation, method 4, wherein relatively small losses in the commutating circuit are assumed, was used.

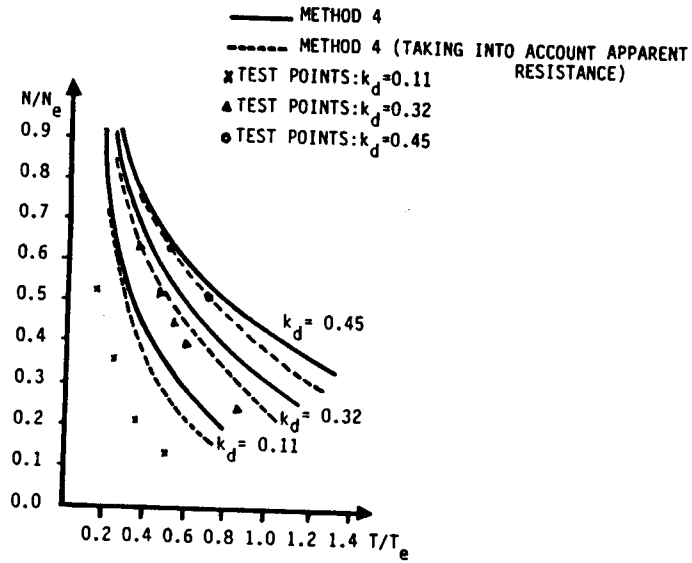

FIGURE 8.10 Speed-torque characteristics of chopper-fed dc motor—Method 4.

8.2.2 Analysis of Inverter-Fed Induction Machine

With the advent of power semiconductor devices, the squirrel-cage induction motor is being used for a variety of industrial applications when variable-speed operation is required. In many of these applications the dynamic behavior of the induction machine has an important effect on the overall performance of the system of which it is a part. Analysis of the dynamic behavior of the ac drive system is quite complex compared to that of a dc drive; the complexity of analysis arises because the equations describing the dynamics of an induction machine are nonlinear. Further, the topology of the power inverter is relatively complex, owing to the presence of a large number of power semiconductor switching elements. It is therefore necessary to make certain simplifying assumptions in order to simulate the inverter and the induction machine using a computer. In addition, to use the computer effectively, it is important to represent the induction machine in a form that holds good for both transient and steady-state conditions. Further, to simplify the analysis of the inverter, a decoupled system is assumed; this enables the inverter output voltage waveforms to be determined independent of the operating conditions of the motor.

The most common representation of the induction machine for the purposes of simulation makes use of the d-q transformation equations. The derivation of the d-q transformation equations for an induction machine is described in Chapter 2. In this section we analyze an ac drive system consisting of an induction motor fed from an inverter operated in different modes. The inverter is modeled

such that the induction motor sees the waveforms as they would be when implemented in a practical system [8].

DYNAMIC EQUATIONS OF INDUCTION MACHINE. For the purpose of analysis, a symmetrical induction machine in a two-axis model is considered. Although any arbitrary reference frame could be used for simulation of an induction machine, let us choose a stationary reference frame for its representation. Recall that the transformation between the d-q variables and the real stator variables is time invariant. The ac drive system is assumed to be a decoupled system; that is, the induction machine is fed from an inverter whose output voltages are independent of the operating modes of the induction machine. Note that the output voltages of the inverter are usually nonsinusoidal.

The machine equations in the stationary reference frame in terms of flux linkages in per unit values are given by

$$\begin{aligned}
\frac{d\phi_{sd}}{dt} &= (v_{sd} - r_s i_{sd})\omega_N \\
\frac{d\phi_{rd}}{dt} &= (-r_r i_{rd} - \omega_r \phi_{rq})\omega_N \\
\frac{d\phi_{rq}}{dt} &= (-r_r i_{rq} + \omega_r \phi_{rd})\omega_N \\
\frac{d\phi_{sq}}{dt} &= (v_{sq} - r_s i_{sq})\omega_N
\end{aligned} \tag{8.29}$$

Note that the transformed stator and rotor flux linkages are given by

$$\begin{aligned}
\phi_{sd} &= L_s i_{sd} + L_m i_{rd} \\
\phi_{rd} &= L_r i_{rd} + L_m i_{sd} \\
\phi_{rq} &= L_r i_{rq} + L_m i_{sq} \\
\phi_{sq} &= L_s i_{sq} + L_m i_{rq}
\end{aligned} \tag{8.30}$$

where

L_s and L_r = stator and rotor self-inductances

L_m = mutual inductance between stator and rotor windings

ω_N = nominal synchronous speed of the rotating magnetic field

The mechanical equation for the drive is given by

$$\frac{d\omega_r}{dt} = \frac{T_e - T_L}{\tau_M} \tag{8.31}$$

where

T_e = electromagnetic torque developed; this is given by

$$T_e = \frac{L_m}{\sigma L_s L_r}(\phi_{sq}\phi_{rd} - \phi_{sd}\phi_{rq}) \tag{8.32}$$

T_L = load torque

ω_r = rotor speed

$\sigma = (L_s L_r - L_m^2)/L_s L_r$

Note that the flux linkages in coupled circuits tend to change more slowly than the currents; therefore, the use of flux linkages provides more computational stability.

The expressions for the transformed currents can be derived using Eq. (8.30); these are given by

$$\begin{aligned}
i_{sd} &= \frac{1}{L_s}\left(\phi_{sd} - \frac{L_m}{L_r}\phi_{rd}\right) \\
i_{rd} &= \frac{1}{L_r}\left(\phi_{rd} - \frac{L_m}{L_s}\phi_{sd}\right) \\
i_{rq} &= \frac{1}{L_r}\left(\phi_{rq} - \frac{L_m}{L_s}\phi_{sq}\right) \\
i_{sq} &= \frac{1}{L_s}\left(\phi_{sq} - \frac{L_m}{L_r}\phi_{rq}\right)
\end{aligned} \tag{8.33}$$

The actual line currents, i_a, i_b, and i_c of the motor are related to the transformed stator currents as given in

$$\begin{aligned}
i_a &= i_{sd} \\
i_b &= \frac{-i_{sd}}{2} + \frac{\sqrt{3}\, i_{sq}}{2} \\
i_c &= \frac{-i_{sd}}{2} - \frac{\sqrt{3}\, i_{sq}}{2}
\end{aligned} \tag{8.34}$$

For the analysis of the induction machine, all the equations derived in this section are used.

SIMULATION OF THREE-PHASE INVERTER OUTPUT VOLTAGE WAVEFORMS. The inverter configuration and the motor connections are shown in Fig. 8.11. The

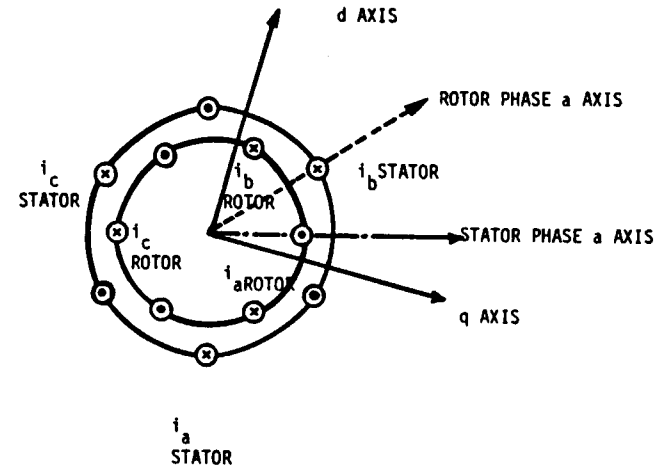

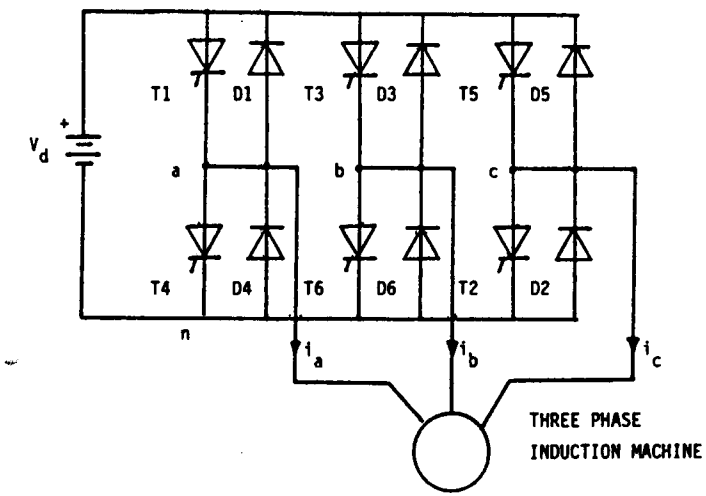

FIGURE 8.11 Three phase inverter and induction machine drive system.

three-phase bridge inverter is operated in such a way that at any instant of time, the poles have defined voltages; that is, at any instant, one of the devices will be conducting in each leg. The motor phase voltages can, therefore, easily be derived; these equations are

$$v_{a0} = \frac{2v_{an} - v_{bn} - v_{cn}}{3}$$

$$v_{b0} = \frac{2v_{bn} - v_{an} - v_{cn}}{3} \qquad (8.35)$$

$$v_{c0} = \frac{2v_{cn} - v_{an} - v_{bn}}{3}$$

For a balanced three-phase supply, the transformed voltages v_{sd} and v_{sq} can be computed using

$$v_{sd} = v_{a0}$$

$$v_{sq} = \frac{v_{bn} - v_{cn}}{\sqrt{3}} \qquad (8.36)$$

Note that Eqs. (8.35) and (8.36) are derived assuming negligible voltage drop in the devices and neglecting the effect of snubber circuits. We now consider three different control strategies for the inverter and derive the corresponding inverter output voltage waveforms:

1. 180° square-wave inverter control
2. Sinusoidal pulse-width-modulated (PWM) inverter control
3. Symmetrical sinusoidal PWM (SSPWM) inverter control

EQUATIONS FOR 180° SQUARE-WAVE INVERTER CONTROL STRATEGY. The output voltage waveforms that are applied to the three-phase induction motor are shown in Fig. 8.12. Referring to Fig. 8.12, we see the following characteristics of inverter operation for this method of control:

1. Semiconductor devices switch sequentially every 60°.
2. At any instant, three semiconductor devices are conducting.
3. Each semiconductor device conducts for a duration of 180°.

The frequency of the inverter is varied by varying the frequency of switching of the devices; the output voltage of the inverter can be varied by varying the input voltage to the inverter.

Referring to Fig. 8.11, we note that the pole voltage v_{an} is positive when either the thyristor T1 or the diode D1 is conducting. When T1 conducts, the current i_a is positive and when D1 conducts, i_a is negative. This can be stated in the form

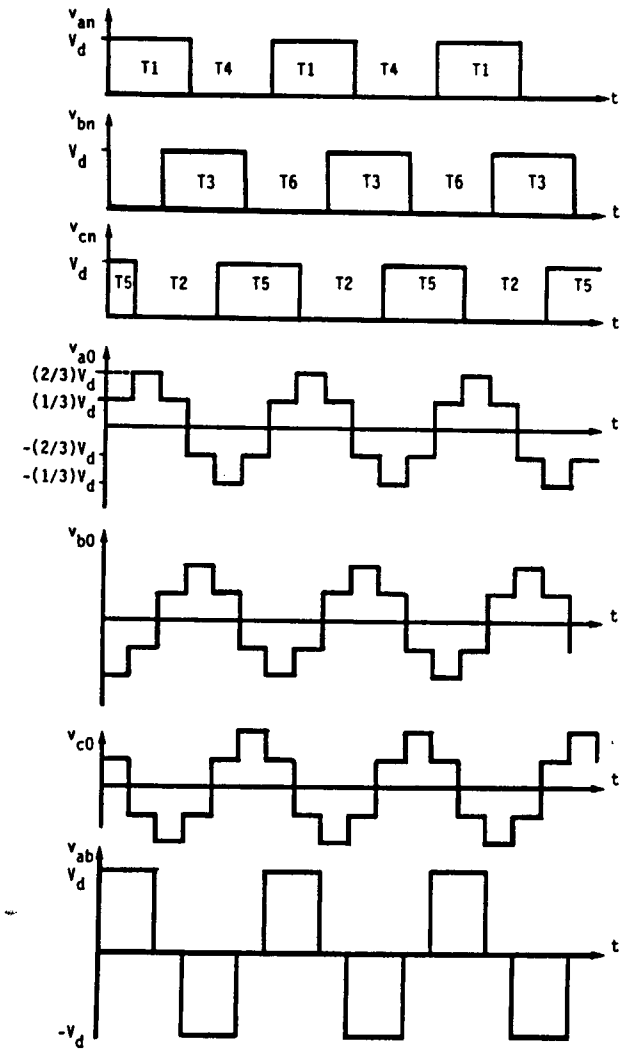

FIGURE 8.12 Output voltage waveforms for 180° mode of operation.

$$v_{an} = \begin{cases} V_d & \text{if T1 or D1 is ON (i.e., TD1 is .TRUE.)} \\ 0 & \text{if T1 and D1 are OFF (i.e., TD1 is .FALSE.)} \end{cases} \quad (8.37)$$

In a similar way, this logic holds good for the other two phases. The dc supply current due to phase a is i_a when TD1 is .TRUE. and is zero when TD1 is .FALSE.. Thus the dc source current can be computed using the logical statement

$$i_{dc} = i_a \cdot TD1 + i_b \cdot TD_3 + i_c \cdot TD_5 \quad (8.38)$$

For implementing the 180° square-wave inverter on the digital computer, the following six states are switched after every 60° at the required frequency of operation of the inverter:

STATE 1: TD1 = .TRUE.; TD3 = .FALSE.; TD5 = .TRUE.
STATE 2: TD1 = .TRUE.; TD3 = .FALSE.; TD5 = .FALSE.
STATE 3: TD1 = .TRUE.; TD3 = .TRUE.; TD5 = .FALSE.
STATE 4: TD1 = .FALSE.; TD3 = .TRUE.; TD5 = .FALSE.
STATE 5: TD1 = .FALSE.; TD3 = .TRUE.; TD5 = .TRUE.
STATE 6: TD1 = .FALSE.; TD3 = .FALSE.; TD5 = .TRUE.

EQUATIONS FOR SINUSOIDAL PWM INVERTER CONTROL. The power circuit configuration for this inverter is the same as that shown in Fig. 8.11, in which either thyristors or transistors can be used. The PWM control strategy is realized by using a high-frequency triangular waveform as the carrier wave and three-phase sinusoidal waveforms as the modulating waves; the intersection points of the triangular waveform with the sinusoidal waveforms define the turn-on and turn-off instants for the six transistors. The inverter output voltage waveforms, v_{an}, v_{bn}, and v_{cn}, are shown in Fig. 8.13. For example, if TD1 is ON when the phase a sine-wave amplitude is greater than the triangular wave (i.e., $v_{an} = V_d$); TD1 is OFF when the amplitude of the phase a sine wave is less than the triangular wave (i.e., $v_{an} = 0$). This logic also holds true for the other two phases.

Let the equations for the three-phase sinusoidal waves be

$$\begin{aligned} v_a &= M \sin \omega t \\ v_b &= M \sin \left(\omega t - \frac{2\pi}{3}\right) \\ v_c &= M \sin \left(\omega t - \frac{4\pi}{3}\right) \end{aligned} \quad (8.39)$$

where M represents the modulation index:

$$M = \frac{\text{amplitude of sine wave}}{\text{amplitude of carrier (triangular) wave}}$$

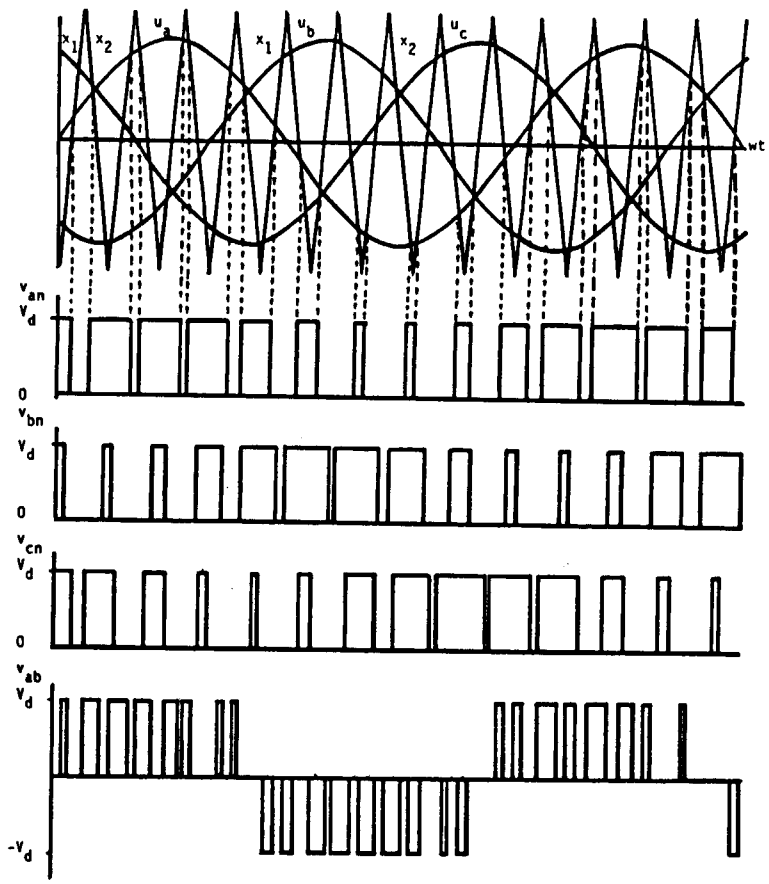

FIGURE 8.13 Output voltage waveforms for sinusoidal PWM inverter.

Further, let the equations for the triangular carrier wave be

$$\begin{aligned} x_1 &= -1.0 + 2N \frac{\omega t}{\pi} \quad \text{for } 0 < \omega t < \frac{\pi}{N} \\ x_2 &= 3.0 - 2N \frac{\omega t}{\pi} \quad \text{for } \frac{\pi}{N} < \omega t < \frac{2\pi}{N} \end{aligned} \quad (8.40)$$

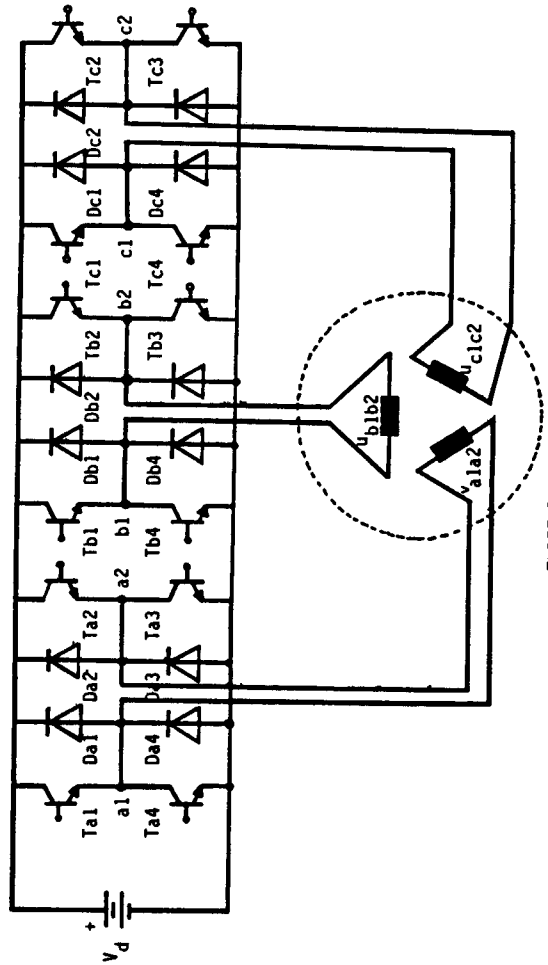

FIGURE 8.14 Three phase induction machine fed by three independent single phase inverters.

For numerical computation of the intersection points, the proper slopes of the triangular waveform are chosen after every interval of π/N. The inverter output voltages are therefore defined as follows:

$$\begin{aligned}
&\text{If } v_a \geq x_1 \text{ or } x_2, \text{ then } v_{an} = V_d \\
&\text{If } v_b \geq x_1 \text{ or } x_2, \text{ then } v_{bn} = V_d \\
&\text{If } v_c \geq x_1 \text{ or } x_2, \text{ then } v_{cn} = V_d \\
&\text{Otherwise, } v_{an} = 0;\ v_{bn} = 0;\ v_{cn} = 0
\end{aligned} \tag{8.41}$$

The expression for the dc source current is similar to Eq. (8.38).

EQUATIONS FOR SSPWM CONTROL STRATEGY. The limitation of the three-phase bridge inverter shown in Fig. 8.11 is that any type of modulation technique cannot be implemented using it, because of the pole switching constraint [8]. Any desired waveform could be applied to the induction machine by feeding each phase of the machine separately by a single-phase bridge inverter. This power circuit configuration is shown in Fig. 8.14. The apparent limitations of the power circuit are:

1. The requirement of a large number of semiconductor devices, resulting in higher cost than for a conventional three-phase bridge configuration
2. The presence of zero-sequence currents in the stator windings

The advantages of the configuration are:

1. Possible implementation of any type of modulation technique without a pole switching constraint
2. Availability of higher output voltage than with a conventional three-phase bridge configuration for the same dc link voltage
3. Possible operation of the devices in order to reduce the switching losses

The induction machine fed from separate inverters as shown in Fig. 8.14 can be modeled by considering it to be similar to a star connection with neutral connected. Equations (8.29) to (8.33) are valid in this case. In addition, an expression for zero-sequence current is required:

$$L_{s0} \frac{di_{s0}}{dt} = (v_{s0} - r_s i_{s0})\omega_N \tag{8.42}$$

Referring to Fig. 8.14, we can derive the relations between the real and the transformed voltages, v_{sd}, v_{sq}, and v_{s0} and v_{a1a2}, v_{b1b2}, and v_{c1c2}:

$$v_{sd} = \frac{2[v_{a1a2} - (v_{b1b2} + v_{c1c2})/2]}{3}$$

$$v_{sq} = \frac{v_{b1b2} - v_{c1c2}}{\sqrt{3}}$$

$$v_{s0} = \frac{v_{a1a2} + v_{b1b2} + v_{c1c2}}{3} \qquad (8.43)$$

The relations between the transformed and the real line currents are given by

$$i_a = i_{sd} + i_{s0}$$

$$i_b = -\frac{i_{sd}}{2} + \frac{\sqrt{3}\, i_{sq}}{2} + i_{s0} \qquad (8.44)$$

$$i_c = -\frac{i_{sd}}{2} - \frac{\sqrt{3}\, i_{sq}}{2} + i_{s0}$$

In the SSPWM control strategy, each pulse width is proportional to the sine of the center point and the width index; further, the pulses are placed symmetrically with respect to the center point, as shown in Fig. 8.15. In simulating these waveforms on a digital computer, the starting and ending instants of each pulse in a half cycle are calculated [8]. Let P_j be the width of the jth pulse, for j = 1 to N:

$$P_j = W \frac{\pi}{N} \sin C_j \qquad (8.45)$$

where

$C_j = \{\pi/N\}(2j - 1)/2$: center point of the jth pulse

N = number of pulses per half cycle

$S_j = C_j - P_j/2$: starting point of the jth pulse

$E_j = C_j + P_j/2$: end point of the jth pulse

In one half-cycle, for phase a, the following relations hold good:

S_j to E_j: $v_{a1a2} = V_d$; Ta1 is .TRUE. and Ta3 is .TRUE.
E_j to S_{j+1} for $(j + 1) < N$: $v_{a1a2} = 0$; Ta1 is .TRUE. and Ta2 is .TRUE.
0 to S_1 and E_N to π: $v_{a1a2} = 0$; Ta1 is .TRUE. and Ta2 is .TRUE.

In another half-cycle,

S_j to E_j: $v_{a1a2} = -V_d$; Ta4 is .TRUE. and Ta2 is .TRUE.
E_j to S_{j+1} for $(j + 1) < N$: $v_{a1a2} = 0$; Ta4 is .TRUE. and Ta3 is .TRUE.
0 to S_1 and E_N to π: $v_{a1a2} = 0$; Ta4 is .TRUE. and Ta3 is .TRUE.

This logic can be extended similarly for phases b and c. The dc supply current is given by

$$i_{dc} = i_{ad} + i_{bd} + i_{cd} \qquad (8.46)$$

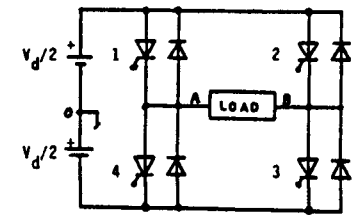

SINGLE PHASE BRIDGE INVERTER

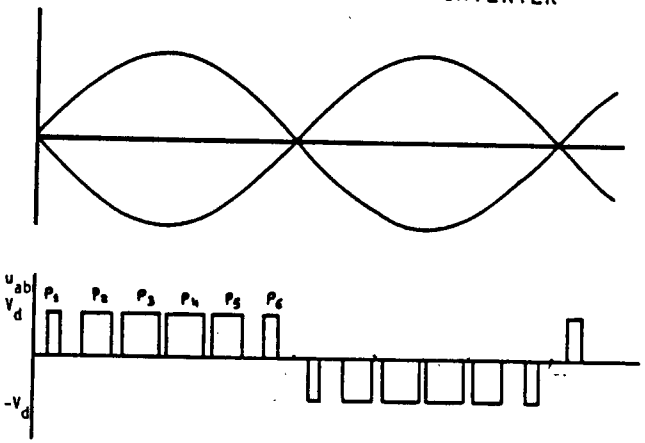

NO. OF DIVISIONS/HALF CYCLE = N = 6
WIDTH OF EACH INTERVAL = 30°
WHEN W = 1,
P_1 = (30) SIN (15) = 7·76°
P_2 = (30) SIN (45) = 21·2°
P_3 = (30) SIN (75) = 28·9°
P_4 = (30) SIN (105) = 28·9°
P_5 = (30) SIN (135) = 21·2°
P_6 = (30) SIN (165) = 7·76°

(THE SINEWAVES ARE DRAWN ONLY FOR REFERENCE)

FIGURE 8.15 SSPWM waveforms for a single phase bridge inverter (N = 6, W = 1).

where,

i_a if Ta1 is .TRUE. and Ta3 is .TRUE.

$i_{ad} = -i_a$ if Ta4 is .TRUE. and Ta2 is .TRUE.

0 if both Ta1 and Ta2 are .TRUE. or Ta4 and Ta3 are .TRUE.

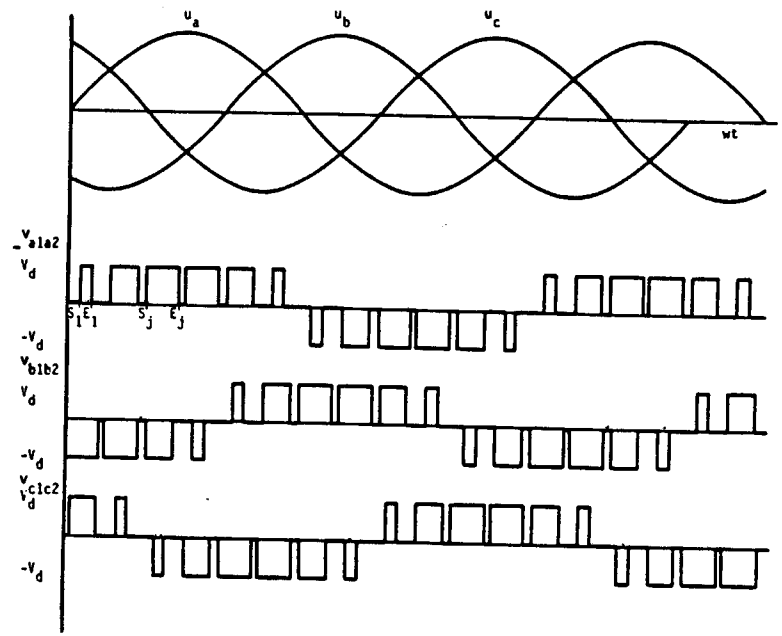

FIGURE 8.16 Output voltage waveforms for SSPWM inverter (N = 6; W = 1).

Note that similar relations hold between i_{bd} and i_b, and between i_{cd} and i_c. Recall that the expression "Ta1 is . TRUE." signifies that either the transistor Ta1 or Da1 in phase a is conducting.

Figure 8.16 shows the output voltage waveforms for the SSPWM inverter.

DIGITAL COMPUTER SIMULATION OF INVERTER-FED INDUCTION MACHINE. It is possible to develop a simulation program which would be able to generate the required output voltage waveforms; further, it would compute the corresponding transformed voltages with a view to calculating the performance characteristics of the induction machines. The generalized flowchart applicable to all three types of inverter control strategy discussed previously is shown in Fig. 8.17. The flowchart indicates the required steps for computation of the free-acceleration characteristics of the induction motor when fed from different nonsinusoidal voltage sources during acceleration and steady-state operation. The input data required are the equivalent-circuit parameters of the induction machine in per unit quantities: frequency, supply voltage, load torque, and number of pulses per half cycle for PWM inverters. The transformed voltages v_{sd} and v_{sq} are computed after every step length and the

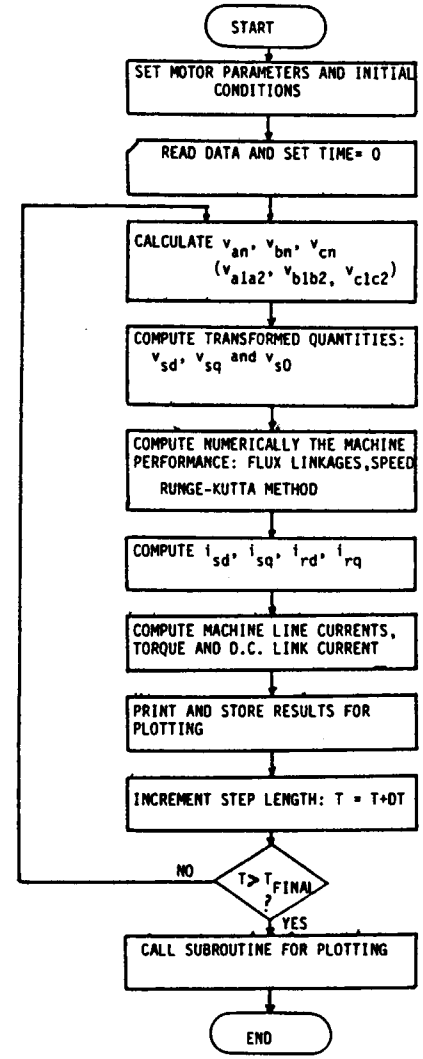

FIGURE 8.17 Flowchart for computation of induction machine performance fed from three phase inverter.

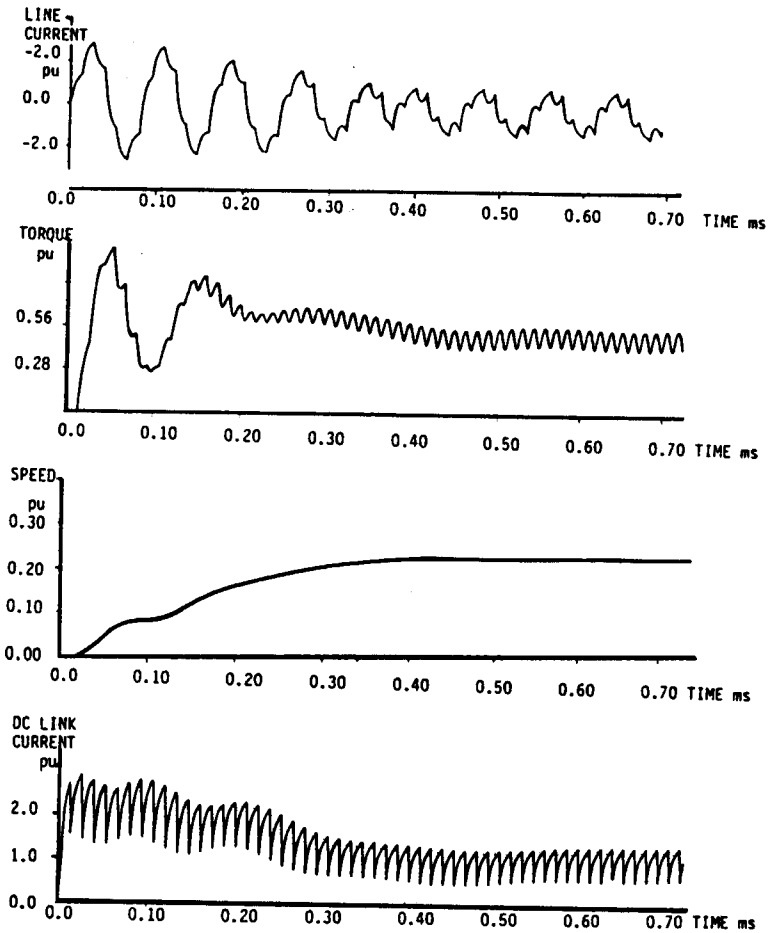

FIGURE 8.18 Computed waveforms for induction machine fed from square wave inverter—180° conduction.

machine equations are solved numerically. The step length used for a square-wave inverter is

$$DT = \frac{1.0}{6f(50)}$$

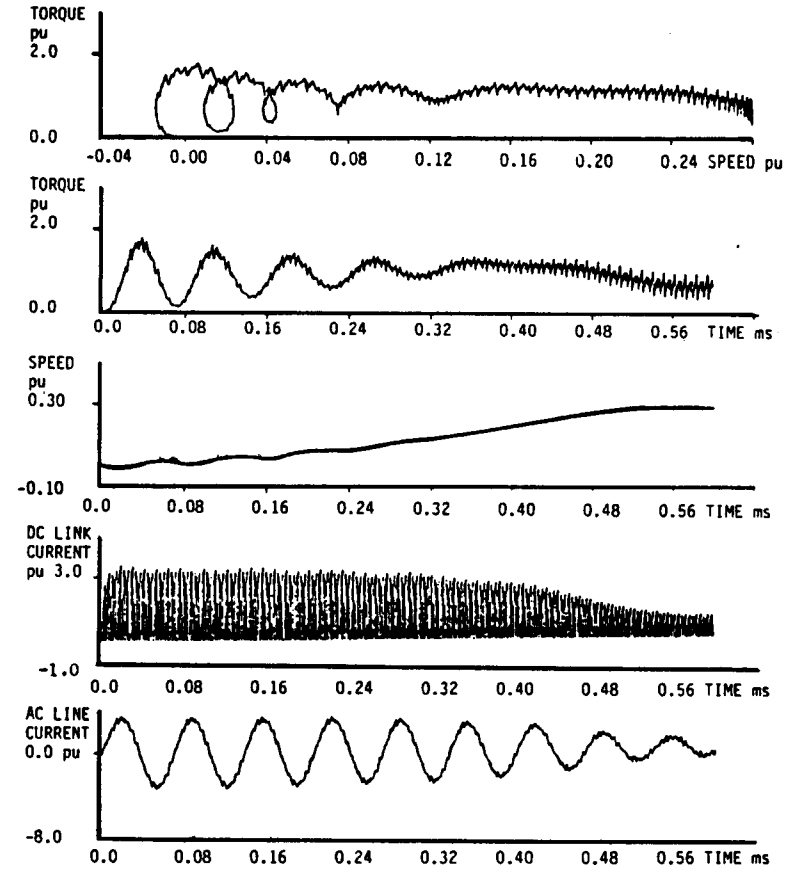

FIGURE 8.19 Computed waveforms for induction machine fed from sinusoidal PWM inverter.

so that there are 50 points in every one-sixth of a period. For PWM and SSPWM inverters, the step length is 60 μs, which is much less than the minimum pulse width.

The typical computed waveforms under different operating conditions are shown in Figs. 8.18, 8.19, and 8.20; these figures show motor line current, torque, inverter input current, and speed as functions of time and torque versus speed. In all cases the ratio of voltage to frequency is kept constant. The circles in the torque-speed characteristics shown in Fig. 8.19 and in Fig. 8.20

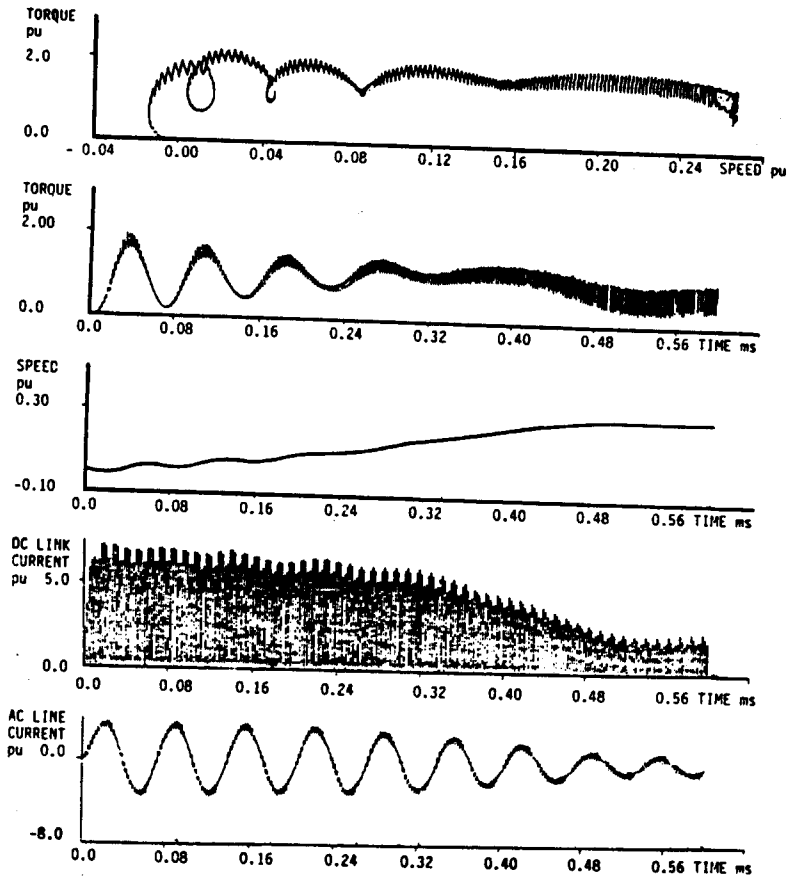

FIGURE 8.20 Computed waveforms for induction machine fed from SSPWM inverter.

are due to the speed oscillations. In these cases the load torque has been kept constant at a value of 0.65 pu. The base quantities and induction machine parameters are given in Table 8.1.

The simulation technique presented here can also be used to study other dynamic characteristics, such as a sudden increase in load, behavior during abnormal operating conditions such as switching off, single phasing, and so on.

TABLE 8.1 Base Quantities and Motor Parameters

Machine:	Three phase induction machine: 2.2 kW, 50 Hz, 400 V, star-connected
Base Quantities:	
Phase voltage:	$V_N = 2\,V_{rms} = 325$ V
Phase current:	$I_N = 2\,I_{rms} = 6.36$ A
Synchronous frequency:	$\omega_N = 314.15$ rad/sec
Flux linkage :	$\phi_N = V_N/\omega_N = 1.034$ Volt sec
Power:	$P_N = 1.5\,V_N\,I_N = 3.1$ kW
Mechanical angular speed:	$\Omega_N = w_N/P = 314.15$ rad/sec
Torque:	$M_N = P_N/w_N = 9.869$ Nm
Impedance:	$Z_N = V_N/I_N = 51.1$ Ohms
Inductance:	$L_N = O_N/I_N = 0.1625$ H
Motor parameters:	
r_s:	0.0684 pu
r_r:	0.02485 pu
L_s:	2.67 pu
L_r:	2.67 pu
L_m:	2.5846 pu
T_s:	0.124 sec
T_r:	0.341 sec
T_m:	0.636 sec
$\sigma = (L_s L_r - L_m^2)/L_s L_r$	

8.3 ANALYSIS OF COUPLED SYSTEMS

For our study we consider the most commonly used ac drive systems using three-phase synchronous and induction machines. In order to provide variable-speed operation of these machines, a variable-frequency power supply is required. This power conversion is usually obtained from a constant-frequency supply mains by the use of a group of converters; for example, a three-phase rectifier supplies a

variable dc voltage or variable dc current output, and a three-phase voltage source or current source inverter provides a variable-frequency power supply.

Earlier we considered a voltage source inverter-fed ac machine and analyzed its performance as a decoupled system. In this section we discuss the case of coupled systems that arise when a current source inverter feeds an ac machine. For the analysis, we consider two cases:

1. A synchronous machine supplied from a naturally commutated inverter
2. An induction machine supplied from a forced-commutated current source inverter.

We first establish the equations describing the operating conditions of the two systems. Then we discuss a generalized procedure for developing a computer-aided analysis program that would enable us to study the various types of ac drive systems using synchronous or induction machines.

8.3.1 Synchronous Machine Fed from a Naturally Commutated Inverter

We consider a balanced three-phase synchronous machine with the stator windings connected in delta; the synchronous machine is fed from a dc current source through a three-phase naturally commutated inverter (NCI). The firing signals for the thyristors are obtained from a rotor position sensor in such a way that operation of the converter is in the naturally commutated inverter mode. Figure 8.21 shows the schematic diagram of the synchronous machine-converter system.

EQUATIONS OF THE SYNCHRONOUS MACHINE-CONVERTER GROUP. For the analysis, the real machine quantities are transformed into d-q quantities. Derivations of these transformed equations are available in Chapter 2. For the

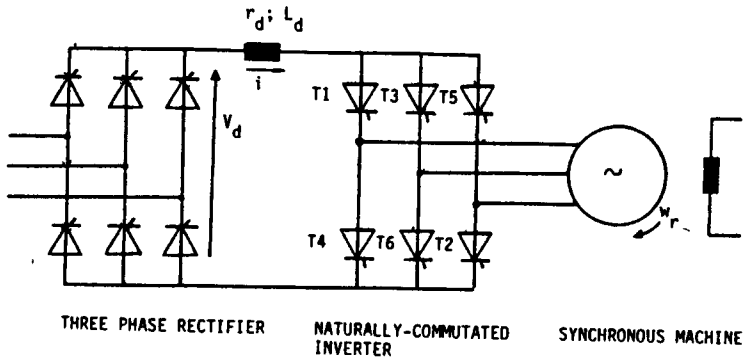

FIGURE 8.21 Synchronous machine—naturally-commutated inverter system.

transformation, a stationary d-q frame is used; further, the d-axis is assumed to be coincident on the stator phase a-axis. The dynamics of the machine can be described by

$$\begin{bmatrix} v_{sd} \\ v_{sq} \\ v_{rd} \\ v_{rq} \end{bmatrix} = \begin{bmatrix} r_s + L_s p & 0 & M_{sr} p & 0 \\ 0 & r_s + L_s p & 0 & M_{sr} p \\ M_{sr} p & M_{sr} \omega_r & r_r + L_r p & L_r \omega_r \\ -M_{sr} \omega_r & M_{sr} p & -L_r \omega_r & r_r + L_r p \end{bmatrix} \begin{bmatrix} i_{sd} \\ i_{sq} \\ i_{rd} \\ i_{rq} \end{bmatrix} \tag{8.47}$$

where

r_s, r_r = stator and rotor resistances

L_s, L_r = stator and rotor self-inductances

M_{sr} = mutual inductance between stator and rotor windings

ω_r = rotor speed of an equivalent two-pole machine

p = differential operator d/dt

The torque equation for the system is given by

$$J \frac{d\omega_r}{dt} + f\omega_r + PT_L = P^2 M_{sr}(i_{rd} i_{sq} - i_{rq} i_{sd}) \tag{8.48}$$

where

P = number of pole pairs

T_L = load torque

J = total inertia of the system

f = frictional coefficient of the load

ω_r = rotor speed of an equivalent two-pole machine

Note that Eq. (8.47) can be obtained from the general equation (2.50); to obtain Eq. (8.47), ω_d is made zero in Eq. (2.50), since the d-q axes are stationary. The synchronous machine fed by the NCI is a coupled system since we take into account the commutation interval of the thyristors. Further, let us take into consideration the dc link inductance L_d and the resistance r_d. In the naturally commutated mode of operation, we can associate 12 sequences of operation in a period, as shown in Fig. 8.3. This would therefore require 12 sets of equations if no further assumptions are made. However, we can note that the three-phase bridge converter exhibits cyclic operation, in which there are only two sequences of operation for a given set of thyristors. For example, in the first sequence of operation, called the "sequence between commutations," thyristors 1 and 6 conduct initially. When thyristor 2 is turned on, the second sequence of operation begins; this is characterized by simultaneous conduction of thyristors 6, 1, and 2. This sequence

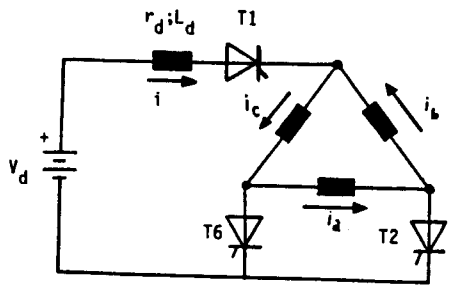

SEQUENCE DURING COMMUTATION

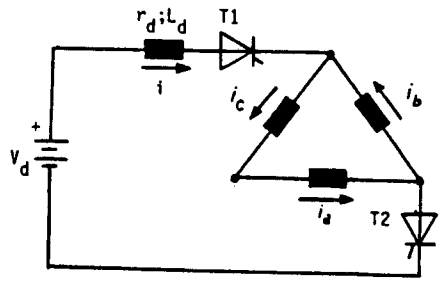

SEQUENCE BETWEEN COMMUTATIONS

FIGURE 8.22 Operating sequences for NCI-fed synchronous machine.

is called the "sequence during commutation." Figure 8.22 shows the operating conditions of the circuit during the two operating sequences. The same two operating sequences occur in a cyclic manner for the other sets of thyristors, with a phase difference of 60°. If we take into account this cyclic operation, it is sufficient to write only two sets of equations describing the dynamics of the coupled system which is applicable for one-sixth of a period.

The dynamic equations for the system during the commutation interval can be calculated:

$$\begin{bmatrix} pi \\ pi_{sd} \\ pi_{rd} \\ pi_{rq} \end{bmatrix} = \begin{bmatrix} \frac{L_r}{U} & \frac{L_r}{\sqrt{6}\,U} & 0 & \frac{M_{sr}}{\sqrt{2}\,U} \\ 0 & \frac{L_r}{S} & \frac{-M_{sr}}{S} & 0 \\ 0 & \frac{-M_{sr}}{S} & \frac{L_s}{S} & 0 \\ \frac{M_{sr}}{\sqrt{2}\,U} & \frac{M_{sr}}{2\sqrt{3}\,U} & 0 & \frac{L_1}{U} \end{bmatrix} \begin{bmatrix} E1 \\ E2 \\ E3 \\ E4 \end{bmatrix} \tag{8.49}$$

where

$$U = L_1 L_r - M_{sr}^2/2$$

$$S = L_s L_r - M_{sr}^2$$

$$L_1 = L_d + L_s/2$$

$$E1 = V_d - (r_d + r_s/2)i - r_s i_{sd}/\sqrt{6}$$

$$E2 = -r_s i_{sd}$$

$$E3 = V_{rd} + M_{sr}\omega_r i/\sqrt{2} - r_r i_{rd} - L_r \omega_r i_{rq}$$

$$E4 = V_{rq} + M_{sr}\omega_r i_{sd} + L_r \omega_r i_{rd} - r_r i_{rq}$$

The dynamic equations for the interval between commutations can be calculated; these equations are the same as those given by Eq. (8.49) with the following differences. The differential equation for i_{sd} in Eq. (8.49) is replaced by

$$\frac{di_{sd}}{dt} = \frac{1}{6}\frac{di}{dt} \tag{8.50}$$

Further, the value of E2 is given by

$$E2 = \frac{E21}{E22} \tag{8.51}$$

where

$$E21 = \sqrt{6}\,L_s L_r SE1 + 6L_s M_{sr} UE3 + \sqrt{3}\,L_s M_{sr} SE4$$

$$E22 = 6US + SL_s L_r + 6UM_{sr}^2$$

Derivation of Eqs. (8.49) to (8.51) is left to the reader as exercises. The torque equation for both the operating sequences is

$$Jp\omega_r = -f\omega_r - PT_L - P^2 M_{sr}\left(\frac{i\, i_{rd}}{\sqrt{2}} + i_{sd} i_{rq}\right) \tag{8.52}$$

8.3.2 Induction Machine Fed from a Forced-Commutated Current Source Inverter

We consider a balanced three-phase induction machine with the stator windings connected in delta; the induction machine is fed from a dc current source through a forced-commutated inverter (FCI). A current source inverter (CSI) configuration is used for the FCI. This configuration uses six main thyristors and six auxiliary thyristors; further, there are three capacitors which are properly charged and discharged during turn-on of the auxiliary and main thyristors; thus they provide the necessary reverse voltage across the main thyristors for their turn-off. Figure 8.23 shows the schematic diagram of the induction machine-converter group.

EQUATIONS OF THE INDUCTION MACHINE-CONVERTER GROUP. For the analysis, once again we use the d-q transformation equations and transform the machine equations into d-q quantities. Let us assume, initially, that the two main thyristors, TM1 and TM6, are conducting. Then thyristors TA6 and TM2 are turned on simultaneously. This will result in instantaneous commutation of main thyristor TM6. Main thyristor TM2 is not turned on, however, because it is still reverse biased. The first sequence of operation of the inverter is characterized

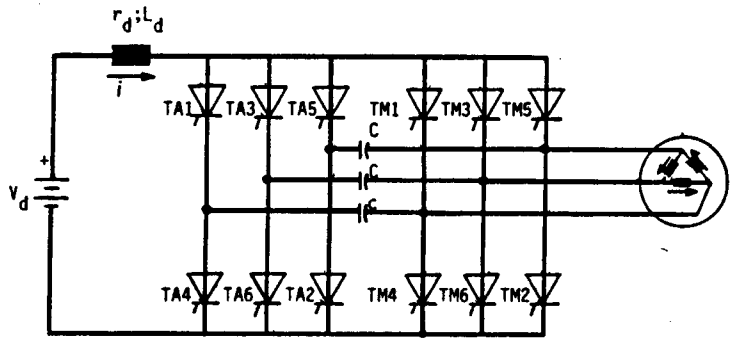

FIGURE 8.23 Current source inverter-fed three phase induction machine.

by charging of the commutating capacitor at constant current as shown in Fig. 8.24. The equations for this sequence are

$$\begin{aligned} i_{sq} &= -\frac{i}{2} \\ i_{sd} &= -\frac{i}{6} \\ V_d &= (r_d + L_d p)i + V_f - \frac{v_{sd}}{6} - \frac{v_{sq}}{2} \end{aligned} \tag{8.53}$$

The second sequence of operation begins when main thyristor TM2 starts conducting. Figure 8.24 shows this operating condition. The corresponding equations are

$$\begin{aligned} i_{sq} &= -\frac{i}{2} \\ v_{sd} &= \frac{3}{2} V_f \\ V_d &= (r_d + L_d p) + V_f - \frac{v_{sd}}{6} - \frac{v_{sq}}{2} \end{aligned} \tag{8.54}$$

The third sequence is characterized by the conduction of only two main thyristors, TM1 and TM2. Figure 8.24 shows this operating condition. The equations describing this sequence are

$$\begin{aligned} i_{sq} &= -\frac{i}{2} \\ i_{sd} &= \frac{i}{6} \\ V_d &= (r_d + L_d p)i + \frac{v_{sd}}{6} - \frac{v_{sq}}{2} \end{aligned} \tag{8.55}$$

It is possible to establish a set of equations that would describe all the three sequences of operation:

$$\begin{bmatrix} pi \\ pi_{sd} \\ pi_{rd} \\ pi_{rq} \end{bmatrix} = \begin{bmatrix} \frac{L_r}{U} & \frac{\epsilon L_r}{U\sqrt{6}} & 0 & \frac{M_{sr}}{\sqrt{2}\,U} \\ 0 & \frac{L_r}{S} & \frac{-M_{sr}}{S} & 0 \\ 0 & \frac{-M_{sr}}{S} & \frac{L_s}{S} & 0 \\ \frac{M_{sr}}{\sqrt{2}\,U} & \frac{\epsilon M_{sr}}{2\sqrt{3}\,U} & 0 & \frac{L_1}{U} \end{bmatrix} \begin{bmatrix} E1 \\ E2 \\ E3 \\ E4 \end{bmatrix} \tag{8.56}$$

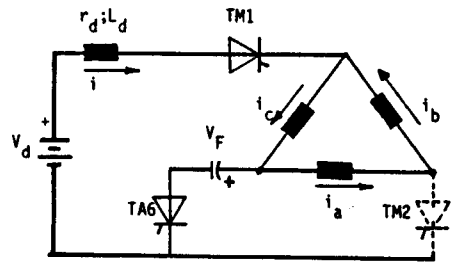

FIRST SEQUENCE

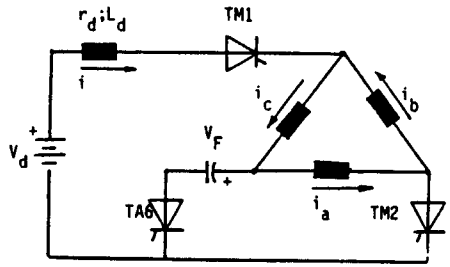

SECOND SEQUENCE

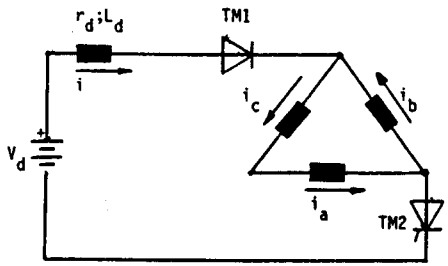

THIRD SEQUENCE

FIGURE 8.24 Operating sequences for CSI-fed induction machine.

Equation (8.56) is applicable to all three sequences, with the following particular conditions:

First sequence:

$$\epsilon = 1$$

$$pi_{sd} = \frac{-\epsilon}{\sqrt{6}} \frac{di}{dt}$$ this replaces the corresponding differential equation in Eq. (8.56)

$$E1 = U - \left(r_d + \frac{r_s}{2}\right) i + \epsilon r_s \frac{i_{sd}}{\sqrt{6}}$$

$$U = V_d - V_f$$

$$E2 = \frac{E23}{E24}$$

$$E23 = 6UL_s M_{sr} E3 - \epsilon\sqrt{6}\, SL_s L_r E1 - \epsilon\sqrt{3}\, L_s M_{sr} SE4$$

$$E24 = 6US + SL_s L_r + 6UM_{sr}^2$$

The expressions for E3 and E4 are the same as those defined for the NCI-fed synchronous machine.

Second sequence:

$$\epsilon = 1$$

$$U = V_d - V_f$$

$$v_{sd} = \frac{\sqrt{3}}{2} V_f$$

$$E2 = \frac{\sqrt{3}}{2} V_f - r_s i_{sd}$$

All other expressions are identical to those described for the first sequence.

Third sequence:

$$\epsilon = -1$$

$$U = V_d$$

All other expressions are identical to those described for the first sequence. Further, for all the sequences, the torque equation is given by Eq. (8.48). We can note that the three sequences have been defined only for one-sixth of the period. Once again, cyclic operation of the various thyristors in the power circuit can be taken into consideration and the analysis need be carried out only for one-sixth of the period.

8.3.3 Computer-Aided Analysis of AC Machine-Converter Group

It is possible to establish a simulation program for the analysis of a power electronic system comprising an ac machine-converter group. Such a general-purpose program has been developed and it is called SECMA [9]. The flowchart for the SECMA simulation program is shown in Fig. 8.25.

The SECMA program permits analysis of various ac drive schemes using either current source inverter (CSI)-fed or voltage source inverter (VSI)-fed ac machines. Table 8.2 lists the subsystems pertaining to the study of VSI-fed ac machines. Table 8.3 shows the subsystems relating to the study of CSI-fed ac machines.

The interesting feature of the SECMA program is that it is possible to study various types of control strategies for the converter-machine group. One example is the use of a speed-regulation loop which does not require a speed sensor [9].

An ac drive scheme using a CSI-fed induction machine is shown in Fig. 8.26. The input current to the CSI is obtained from a three-phase bridge rectifier operated in the current-regulated mode. A proportional-integral (PI) controller has been used for the current control loop. The speed reference values for the input current I_s^* and the speed of the induction motor ω_s^* are computed from

$$\omega_s^* = kv_{sq}$$

$$I_s^* = I_{sn}\sqrt{\frac{\pi}{3\sqrt{2}}\,\frac{1 + L_r^2\omega_r^2}{r_r^2}} \tag{8.57}$$

where I_{sn} represents the stator current corresponding to the nominal value of flux; all other quantities have been defined earlier for the ac machine. The current-source inverter uses only one commutating capacitor but requires six auxiliary thyristors and six main thyristors. The parameters of the machine are shown in Table 8.4. Figure 8.27 shows the starting transient for the induction motor line current, voltage, speed, commutating capacitor voltage, rectifier output current, and motor torque as functions of time. These waveforms have been obtained using the SECMA simulation program.

An examination of the motor line current and voltage in Fig. 8.27 shows a progressive increase in the stator frequency. The rectifier output current is nearly constant during starting. This is ensured by the PI current controller incorporated in the control circuit of the three-phase converter. Figure 8.28 shows the waveforms for a step increase in the stator current reference.

We consider a VSI-fed induction machine in Fig. 8.29. A variable voltage at the input of the VSI is obtained from a dc chopper. Further, the scheme shown in Fig. 8.29 uses an input LC filter at the output of the dc chopper. The speed regulation of the induction machine is done without a speed sensor. The details of a state variable type of controller are shown in Fig. 8.29. Table 8.5 shows the parameters of the ac drive scheme.

Figure 8.30 shows the starting transients of the VSI-fed induction motor. The different waveforms that are plotted are the motor line current, line voltage, inverter input voltage, chopper output current, and motor speed. Note that a

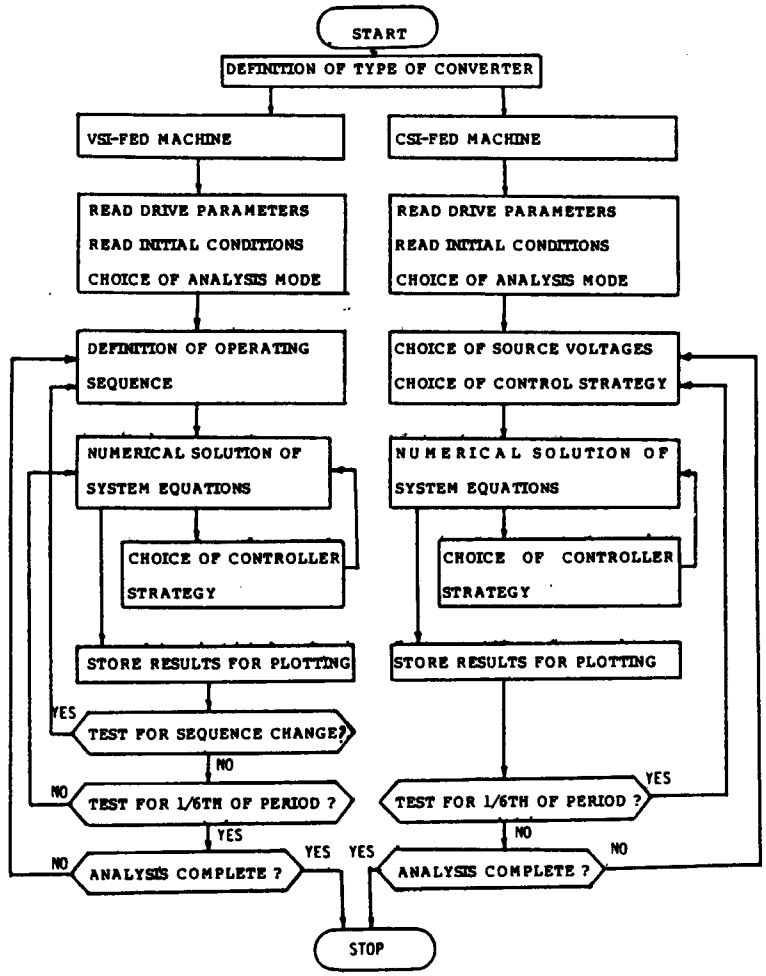

FIGURE 8.25 Flowchart for the SECMA simulation program

TABLE 8.2 SECMA Simulation Subsystems for VSI-fed AC Machines

Types of voltage sources:	1.	d.c. voltage source
	2.	d.c. voltage source-chopper group; with PI current regulator for chopper
	3.	d.c. voltage supplied by a rectifier
Operating inverter modes:	1.	180° conduction
	2.	PWM with constant duty cycle
	3.	PWM with variable duty cycle
	4.	two-level with hysteresis current control
Control strategies:	1.	self-regulated speed control with speed sensor
	2.	speed regulation without speed sensor
Analysis modes:	1.	starting transient
	2.	step change in load torque
	3.	step change in speed reference
	4.	speed reversal transient
	5.	steady state computation

TABLE 8.3 SECMA Simulation Subsystems for CSI-fed AC Machines

Types of current sources:	1.	current-regulated three phase rectifier with PI regulator
	2.	current-regulated three phase rectifier with sampled-data regulator
Control strategies:	1.	speed regulation loop with speed sensor
	2.	speed regulation without speed sensor
Analysis modes:	1.	starting transient
	2.	step variation of current reference
	3.	step variation of load torque
	4.	step variation of speed reference
	5.	step variation of flux
	6.	speed reversal transient
	7.	steady state computation
	8.	motoring-coasting and braking transients

TABLE 8.4 CSI-fed Induction Machine System Parameters

Type of machine:	Slip-ring induction machine
Nominal power:	4.7 kW
Number of Poles:	4
Nominal voltage:	220 V/ 127 V
Nominal line current	20 A/ 35 A
Stator resistance, r_s:	0.0713 Ohm
Rotor resistance, r_r:	0.159 Ohm
Stator self inductance, L_s:	0.0378 H
Rotor self inductance, L_r:	0.0220 H
Mutual inductance, M_{sr}:	0.0278 H
Moment of inertia, J:	0.08 kg m^2
Frictional coefficient, f:	0.04 Nm/rad/sec
D.C. link resistance, r_d:	1 Ohm
D.c. link inductance, L_d:	0.030 H
Commutating capacitance, C_c:	30 μF

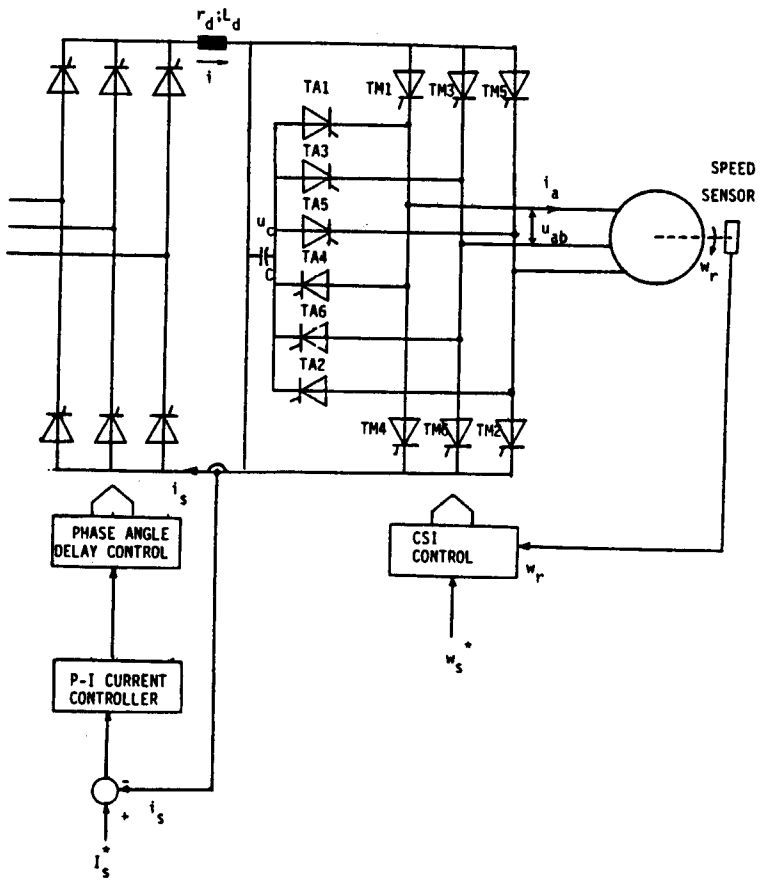

FIGURE 8.26 CSI-fed induction machine ac drive system.

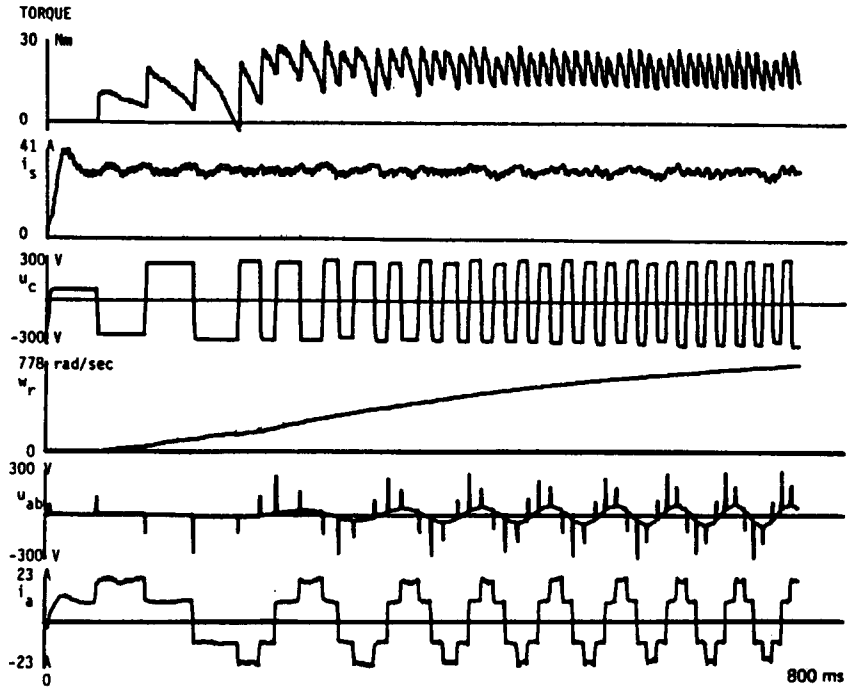

FIGURE 8.27 Starting transients for CSI-fed induction motor.

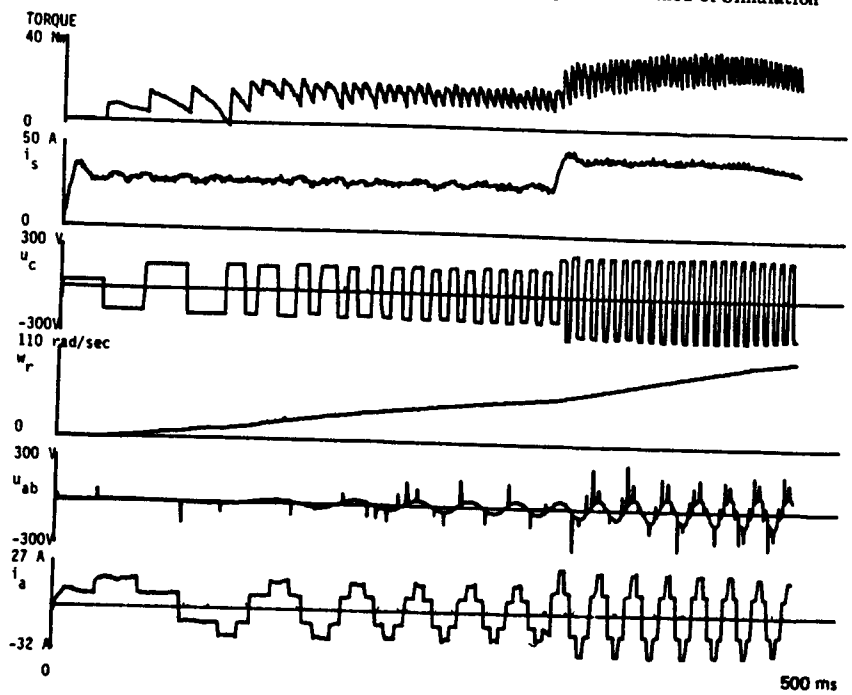

FIGURE 8.28 Step change in I_s^* for CSI-fed induction motor.

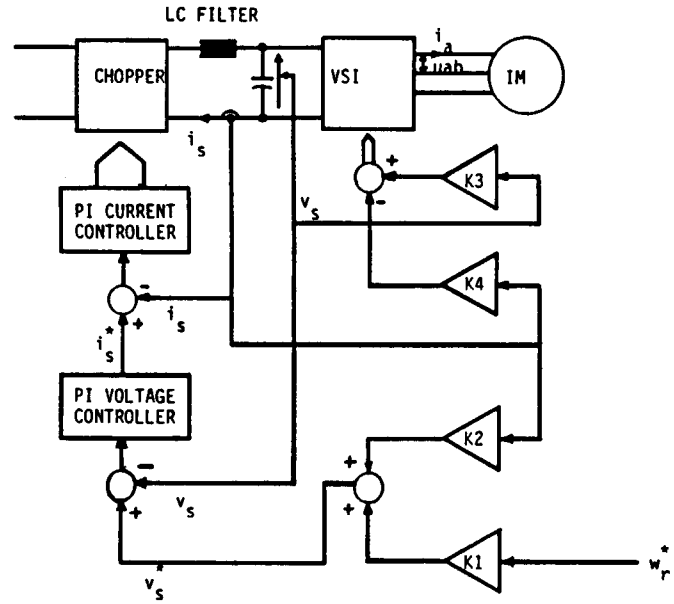

FIGURE 8.29 VSI-fed induction machine ac drive system.

TABLE 8.5 VSI-fed Induction Machine System Parameters

Type of machine:	squirrel-cage induction machine
Nominal power rating:	11 kW
Nominal frequency:	50 Hz
Nominal stator winding voltage:	220 V
Stator resistance, r_s:	0.5 Ohm
Rotor resistance, r_r:	0.5 Ohm
Stator self inductance, L_s:	0.069 H
Rotor self inductance, L_r:	0.069 H
Mutual inductance, M_{sr}:	0.067 H
Moment of inertia, J:	0.08 kg m^2
Frictional coefficient, f:	0.1 Nm/rad/sec
D.C. link filter resistance, r_d:	0.5 Ohm
D.C. link filter inductance, L_d:	0.040 H
D.C. link filter capacitor, C_d:	2000 μF

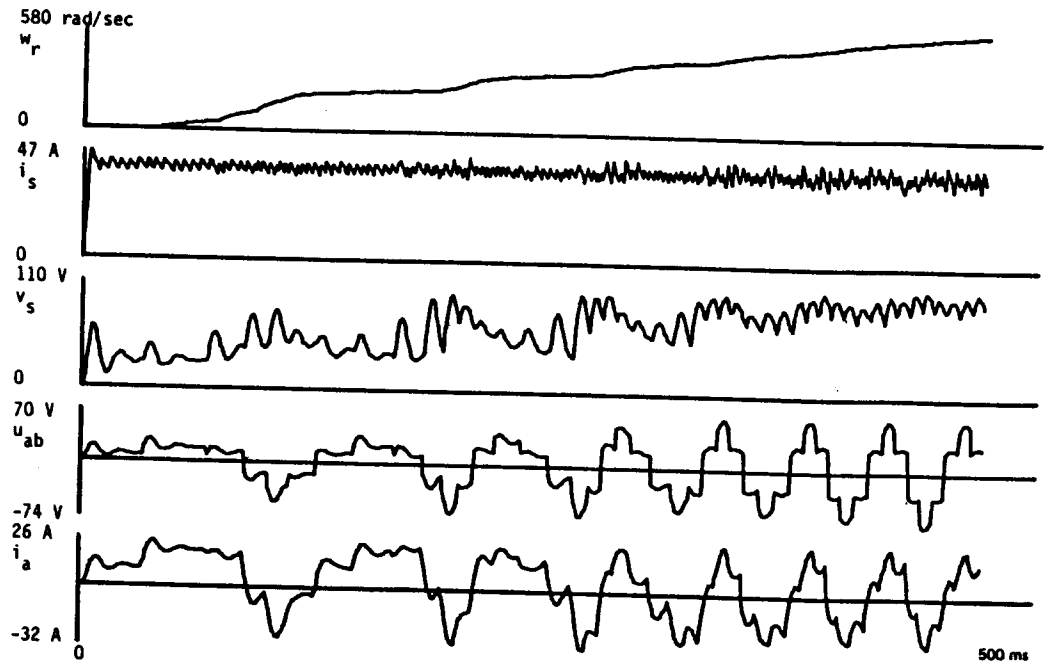

FIGURE 8.30 Starting transients for VSI-fed induction motor.

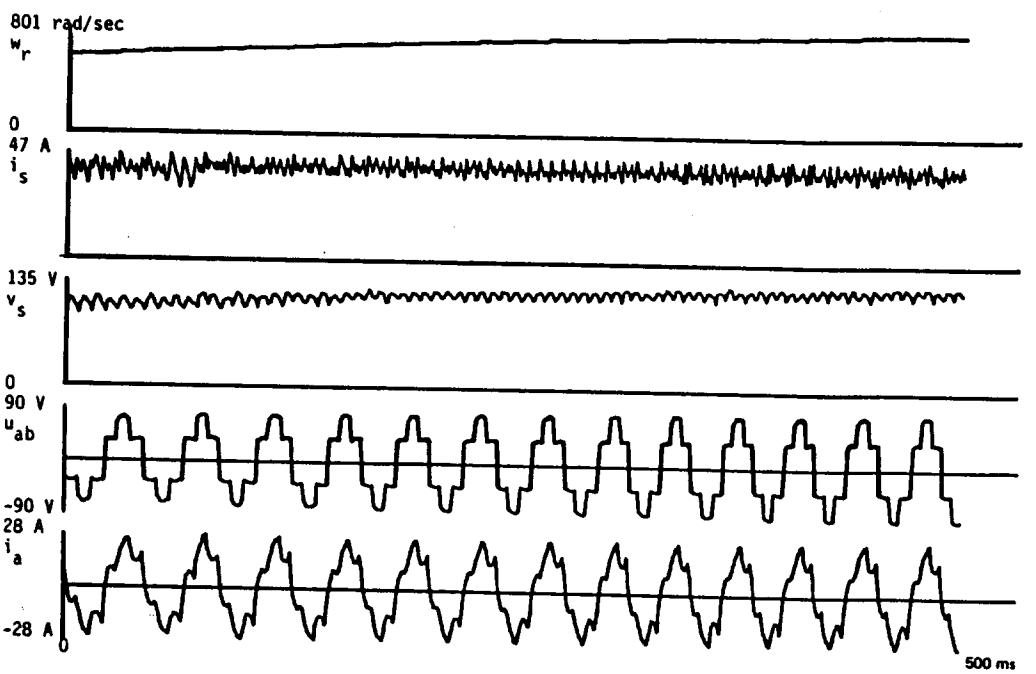

FIGURE 8.31 Step change in reference speed—VSI-fed induction motor.

constant current is maintained at the chopper output during the starting period. This is ensured by the PI regulator in the dc input stage. Figure 8.31 shows the waveforms when there is a step change in the reference speed.

8.4 SUMMARY

Analysis of power electronic converter-electrical machine group has been discussed. The analysis is based on equations established for known set of operating sequences.

In Section 8.1 we discussed two types of systems, decoupled and coupled. In the case of decoupled systems, it is possible to predict the output voltage waveforms independent of the operating conditions of the electrical machine. Usually, decoupled systems arise when the commutation intervals in the operation of the converter are neglected.

Analysis of two examples of decoupled systems was discussed in Section 8.2. The first example covered the chopper-fed dc motor. The analysis of this system was based on the assumption of negligible commutation interval. In the second example we discussed an induction motor fed from a voltage-source inverter. This analysis was based on the d-q transformation equations for the induction machine. Three different control strategies—180° conduction, PWM, and SSPWM—were considered for the inverter control.

In Section 8.3 we considered the case of coupled systems. The first example discussed the case of an ac drive using a synchronous machine and a naturally commutated inverter. In the second example an ac drive using an induction machine and a forced-commutated current-source inverter was discussed. Finally, in Section 8.3.3 we discussed a generalized method of analysis of coupled or decoupled ac drive systems with their associated control strategies.

8.5 REFERENCES

1. V. Rajagopalan, ATOSEC5 Users' Manual, Département d'ingénierie, Université du Québec à Trois-Rivières, Quebec, Canada (August 1985).

2. J. Schonek, Simulation numérique de convertisseurs statiques: Elaboration d'un programme général—Application à la conception et à l'optimisation des convertisseurs (Numerical simulation of statis converters: Elaboration of a general purpose simulation program; application in the design and optimization of converters), Docteur-Ingénieur Thesis, Institut National Polytechnique, Toulouse, France (February 14, 1977).

3. B. Davat, Etude—mise au point et applications d'une méthode de simulation globale de convertisseurs statiques connectés à des charges électriques complexes (Study and development of a global simulation program for the study of converter-fed complex electric loads), Docteur-Ingénieur Thesis, Laboratoire d'electrotechnique et d'électronique industrielle, Toulouse, France (June 27, 1979).

4. Cyril W. Lander, Power Electronics, McGraw-Hill Book Company (U.K.) Ltd., Maidenhead, Berkshire, England, Chap. 3 (1981).

5. R. Parimelalagan and V. Rajagopalan, Steady State Investigations of a Chopper-Fed DC Motor with Separate Excitation, IEEE Transactions on Industry and General Applications, Vol. IGA-7, No. 1, 101-108 (1971).

6. B. D. Bedford and R. G. Hoft, Principles of Inverter Circuits, John Wiley & Sons, Inc., New York, Chap. 10 (1964).

7. K. Heumann, Pulse control of dc and ac motors by silicon-controlled rectifiers, IEEE Transactions on Communications and Electronics, Vol. 83, July, 390-399 (1964).

8. K. S. Rajashekara, Investigations on improved techniques for voltage source inverter-fed induction motor control, Ph. D. thesis, Indian Institute of Science, Bangalore, India (1983).

9. German Cruz Jovanne, Etude et mise au point d'un programme de simulation numérique par séquences (SECMA) d'ensembles constitués de convertisseurs statiques et de machines à courant alternatif. Application à la simulation de variateurs electrotechnique et d'électronique industrielle, Toulouse, France (February 22, 1982).